Clim Dyn (2016) 47:2331–2343
DOI 10.1007/s00382-015-2966-6

Predictability of winter temperature in China from previous autumn Arctic sea ice

Jinqing Zuo[1,3] · Hong-Li Ren[1,4] · Bingyi Wu[2] · Weijing Li[1,3]

Received: 22 July 2015 / Accepted: 22 December 2015 / Published online: 8 January 2016

Abstract The potential predictability of winter temperature in China from autumn Arctic sea ice anomalies is studied by examining and statistically modeling the large–scale interannual covariability between them on the basis of singular value decomposition analysis. It is demonstrated that an intimate relationship exists between September and October sea ice anomalies in the Eurasian Arctic and following winter temperature anomalies in China, except in the Tibetan Plateau. When the autumn sea ice anomalies decline in the Eurasian Arctic, above-normal pressure anomalies appear to prevail over the region from the Eurasian Arctic to Eastern Europe and Mongolia, and below-normal anomalies prevail over the mid-latitudes of Asia and Northwestern Pacific in the following winter. Consequently, the winter Siberian High and East Asian trough are both strengthened, favoring the southward invasion of high–latitude cold air masses and thus cold temperature anomalies in China. It is found that the Siberian High plays a crucial role in delivering effects of the autumn Arctic sea ice anomalies on winter temperature variability in China. Based on this evidence, a statistical model is established to examine the potential predictability of winter temperature anomalies in China by taking the autumn Arctic sea ice signals as a predictor. Validation shows considerable skill in predicting winter temperature anomalies over a large part of China, indicating a significant potential for improving winter climate prediction in China.

Keywords Autumn Arctic sea ice · Surface air temperature · Siberian High · Arctic Oscillation · Predictability

1 Introduction

Observational evidence shows that the Arctic sea ice cover has rapidly declined in the past three decades (Bader et al. 2011), and this decline has been accelerating since the late 1990s (Comiso et al. 2008; Comiso 2012), which is dynamically consistent with decadal changes in the Arctic surface wind pattern in summer and previous spring and winter (Ogi et al. 2010; Wu et al. 2012). Observational and numerical studies have demonstrated that the Arctic sea ice decline could exert substantial impact on the remote large–scale atmospheric circulation and surface weather and climate in the extratropical Northern Hemisphere (Budikova 2009; Bader et al. 2011; Vihma 2014; Gao et al. 2015).

The below-normal sea ice anomalies in the North Atlantic sector of the Arctic tend to induce a negative phase of the Arctic Oscillation/North Atlantic Oscillation (AO/NAO) during winter (Alexander et al. 2004; Deser et al. 2004, 2007; Nakamura et al. 2015), which favors cold temperature anomalies over Northern Eurasia and with the converse also true. Although global warming has continued (Karl et al. 2015), regional extreme cold winter events have frequently occurred over Eurasia in the past several years,

✉ Hong-Li Ren
renhl@cma.gov.cn

1 Laboratory for Climate Studies, National Climate Center, China Meteorological Administration, 46 Zhongguancun Nandajie, Beijing 100081, China

2 Chinese Academy of Meteorological Sciences, Beijing 100081, China

3 Collaborative Innovation Center on Forecast and Evaluation of Meteorological Disasters, Nanjing University of Information Science and Technology, Nanjing 210044, China

4 Joint Center for Global Change Studies (JCGCS), Beijing 100875, China

which can likely be attributed to the Arctic sea ice decline in the preceding summer–autumn seasons, as revealed by previous studies (Petoukhov and Semenov 2010; Wu et al. 2013; Tang et al. 2013; Mori et al. 2014).

It has been indicated that the variability in the East Asian winter climate is closely related to the autumn–winter sea ice anomalies in the Arctic. The autumn–winter sea ice decline in the Atlantic–Eurasian sector of the Arctic tends to enhance the East Asian winter monsoon (EAWM) and results in cold winter temperature anomalies in East Asia (Wu et al. 1999, 2011; Honda et al. 2009). In addition, sea ice anomalies in the Pacific sector have a significant influence on the variability in the EAWM and the East Asian surface climate in winter (Liu et al. 2007; Li and Wang 2013). Liu et al. (2012) recently pointed out that the autumn Arctic sea ice decline may favor a snowy winter in northern and central China. Results from observations and model simulations have suggested that the Arctic sea ice minimum in autumn 2007 was a key factor in the extremely long-lasting series of snowstorm events in January 2008, which severely affected China (Wu et al. 2011; Liu et al. 2012). Therefore, the autumn Arctic sea ice anomalies act as an important predictor of winter precipitation anomalies (Liu and Ren 2015) and may provide an implication for the skillful prediction of winter temperature anomalies in China (Koenigk et al. 2015).

Different mechanisms responsible for the linkage between autumn Arctic sea ice and East Asian winter climate anomalies have been put forward. Honda et al. (2009) found that the September sea ice decline along the Siberian coast tends to accompany cold temperature anomalies over the Far East in the following winter. However, the associated mechanisms differ between early and later winters. The former is related to an intensified Siberian High (SH), while the latter is linked to the negative phase of the NAO. Wu et al. (2011) confirmed the intimate relationship between winter SH and autumn sea ice anomalies in the central Arctic Ocean and Siberian marginal seas, whereas Li and Wu (2012) revealed a significantly in-phase relationship between winter AO and autumn pan-Arctic sea ice area anomalies. In contrast, Liu et al. (2012) showed that the pattern of winter atmospheric circulation anomalies associated with the autumn Arctic sea ice anomalies show different spatial characteristics and interannual variability from the classical AO pattern, which is further supported by Mori et al. (2014). Other studies have suggested that the pattern of atmospheric circulation response appears to depend on the strength and position of the sea ice anomalies in the Arctic (Alexander et al. 2004; Rinke et al. 2013; Koenigk et al. 2015). For example, Alexander et al. (2004) revealed that the large–scale atmospheric response to ice extent anomalies in the North Atlantic sector of the Arctic resembles the AO/NAO pattern, but the atmospheric response to ice extent anomalies in the Sea of Okhotsk is presented as a wave train extending downstream over North America during winter.

Therefore, on one hand, the mechanism responsible for the linkage between autumn Arctic sea ice and the following winter East Asian climate variability remains controversial and unclear. On the other hand, the sea ice anomalies in different regions of the Arctic may have distinct effects on the overlying atmospheric circulation and remote surface climate variability (Alexander et al. 2004; Rinke et al. 2013; Koenigk et al. 2015). These motivate us to further understand the typical features and possible mechanisms of the linkage between autumn Arctic sea ice anomalies and the following East Asian winter climate variability. This study aims to investigate the large–scale patterns of interannual covariability between winter temperature anomalies in China and autumn sea ice anomalies in the Arctic using a singular value decomposition (SVD) technique and further explores the associated physical mechanism. More importantly, we also examine the potential predictability of winter temperature anomalies in China from the autumn Arctic sea ice variations by establishing a statistical prediction model.

The remainder of this paper is organized as follows. Section 2 describes the data and methods used in this study. Section 3 presents the SVD analysis results regarding the relationship between winter temperature anomalies in China and the previous autumn sea ice anomalies in the Arctic. The associated possible mechanism is explored in Sect. 4. Section 5 further investigates the potential predictability of winter temperature anomalies in China from the autumn Arctic sea ice variations, followed by conclusions and discussion in Sect. 6.

2 Data and method

This study uses observations of monthly surface air temperature for 160 Chinese stations provided by the National Climate Center of China Meteorological Administration (http://ncc.cma.gov.cn/Website/index.php?ChannelID=43&WCHID=5). These data are available from 1951 to present. The geographic locations of the 160 stations are shown in Fig. 2c. It should be noted that there are no stations over the western Tibetan Plateau. The Cressman interpolation technique is performed on the station data to arrive at a final product with a horizontal resolution of 1° × 1°. Additionally, the monthly sea ice concentrations are provided by the Met Office Hadley Centre and have a horizontal resolution of 1° × 1° for the period of 1870–2014 (Rayner et al. 2003). The monthly geopotential height, air temperature, and zonal and meridional wind components with a horizontal resolution of 2.5° × 2.5° are derived from

the National Centers for Environmental Prediction/Department of Energy (NCEP/DOE) Reanalysis II for the period of 1979–2014 (Kanamitsu et al. 2002). In addition, the monthly sea level pressure (SLP) with a horizontal resolution of approximately 1.875° × 1.875° is obtained from the NCEP/DOE Reanalysis II. Because the satellite coverage of sea ice starts in 1979, we mainly focus on the period of 1979–2014 in this study. Winter mean is generated as the December–January–February average.

The monthly AO and NAO indices used in this study are obtained from the National Oceanic and Atmospheric Administration/Climate Prediction Center (http://www.cpc.ncep.noaa.gov/). Here, the NAO index is constructed by a rotated principal component analysis with the monthly mean standardized 500-hPa height anomalies poleward of 20°N (Barnston and Livezey 1987). Following Wu and Wang (2002), the SH intensity index is defined as the regional-averaged SLP anomalies over 40°–60°N and 80°–120°E. To focus on interannual variability, linear trends in the time series of temperature and sea ice, except those shown in Fig. 1, have been removed prior to our analysis.

In this study, the statistical significance of regression and correlation coefficients is assessed using a two-tailed Student's t test, where the serial correlation (Zwiers and von Storch 1995) is not taken into account when deducing significance levels.

3 SVD analysis linking Arctic sea ice and temperature in China

Arctic sea ice grows in boreal autumn–winter seasons with anomalies that are characterized by strong interannual variability. In turn, these anomalies can have considerable effect on the overlying atmosphere inducing variability in remote surface climate. Thus, the climatological characteristics and variations of autumn sea ice in the Arctic are investigated prior to analysis of their relationship with winter temperature anomalies in China. Figure 1 shows the climatological means and standard deviations of the monthly Arctic sea ice for September to November for the period of 1979–2014. In September, the central Arctic Ocean and the

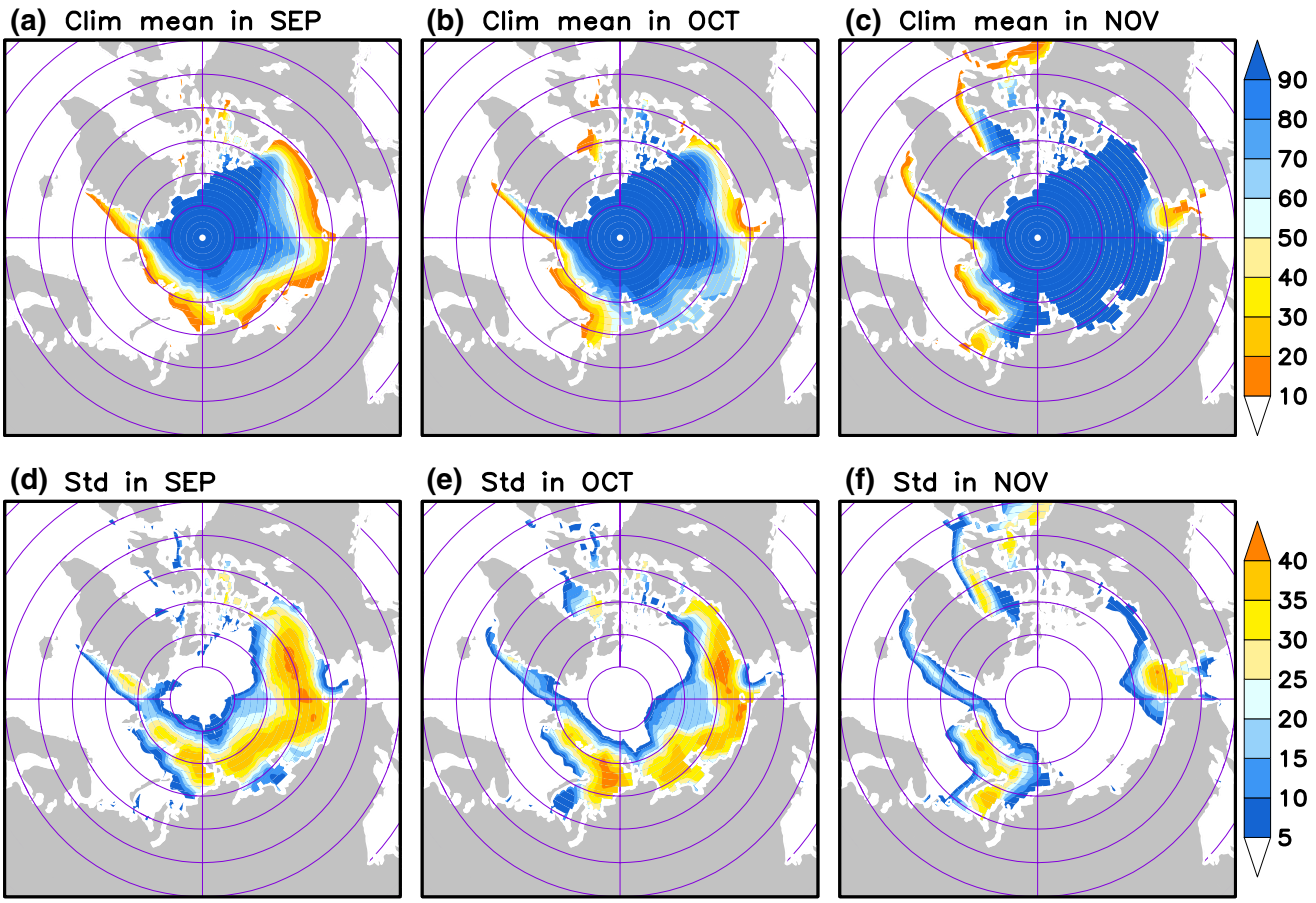

Fig. 1 Climatological mean of Arctic sea ice concentration in **a** September, **b** October and **c** November for the period of 1979–2014. **d**–**f** The same as **a**–**c**, but for the standard deviation. The unit is %

north coasts of Greenland and Canada are nearly entirely covered with sea ice (Fig. 1a), and only the sea ice in the other marginal seas of the Arctic shows large variations (Fig. 1d). The Arctic sea ice cover extends slightly southward in October compared with that in September (Fig. 1b, e). In November, the sea ice cover moves further southward (Fig. 1c), whereas only that in the Atlantic and Pacific sectors of the Arctic still exhibits large variations (Fig. 1f).

An SVD technique is applied to extract large–scale patterns of interannual covariability between winter-mean temperature anomalies in China and monthly sea ice anomalies in the Arctic (69.5°–87.5°N) for September to November. We show the heterogeneous correlation maps of the temperature anomalies and homogeneous correlation maps of the sea ice anomalies associated with the first leading SVD mode in this study because the other modes show less significance.

Figure 2a, b show the spatial patterns of the first SVD mode between winter temperature anomalies in China and September sea ice anomalies in the Arctic. This mode explains approximately 73 % of the total covariance, and the correlation coefficient (R) between the temporal expansion coefficients is 0.76 (Fig. 3a), which is significant at the 99 % confidence level (Table 1). The winter temperature pattern primarily features significant and positive heterogeneous correlations in China, except in the Tibetan Plateau (Fig. 2a), which highly resembles the first leading empirical orthogonal function (EOF) pattern of winter temperature anomalies in China (Fig. 4). The associated September sea ice pattern has significant and positive homogeneous correlations along the Siberian coast, including the region from the Barents Sea eastward to the Laptev sea (Fig. 2b).

Also, the first SVD mode between winter temperature anomalies in China and October sea ice anomalies in the Arctic is identified, which explains approximately 67 % of the total covariance (Table 1). The winter temperature pattern associated with the October sea ice anomalies (Fig. 2c) resembles that associated with the September sea ice anomalies. In addition, the spatial patterns of October and September sea ice anomalies are similar (Fig. 2b, d).

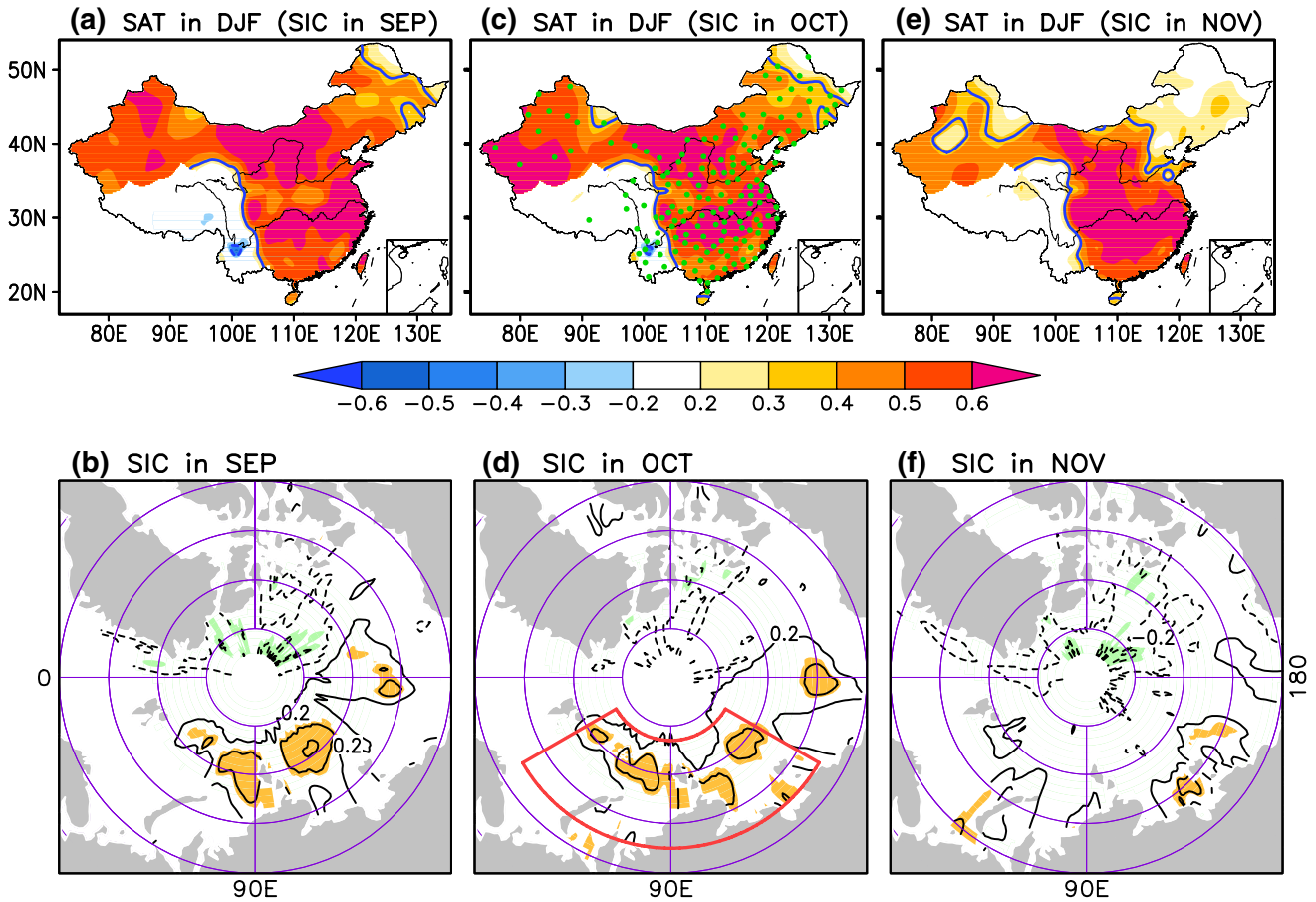

Fig. 2 Spatial patterns of the first SVD mode between detrended **a** winter temperature anomalies in China and **b** September sea ice anomalies in the Arctic for the period of 1979/80–2013/14. *Blue* contour in (**a**) and *shading* in (**b**) indicate significance at the 95 % confidence level. **c**, **d** and **e**, **f** the same as **a**, **b**, but for the sea ice anomalies in October and November, respectively. *Dots* in (**c**) show the geographic locations of the 160 stations in China

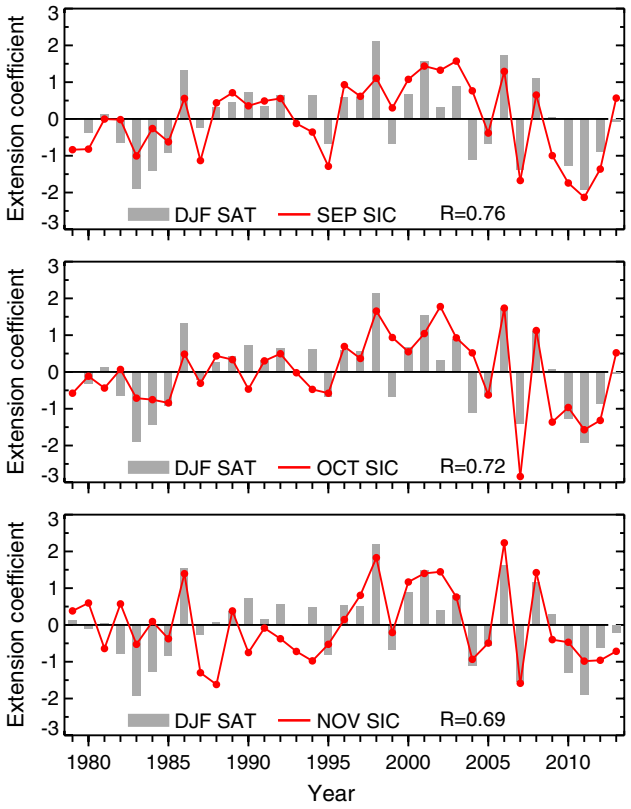

Fig. 3 Expansion coefficients of the first SVD mode between detrended **a** winter temperature anomalies in China (*grey bar*) and **b** September sea ice anomalies in the Arctic (*red line*) for the period of 1979/80–2013/14. **c**, **d** and **e**, **f** the same as **a**, **b**, but for the sea ice anomalies in October and November, respectively

Table 1 Squared covariance fraction (SCF) and temporal correlation coefficient (*R*) between the expansion coefficients of the first SVD mode between detrended winter (December–January–February) temperature anomalies in China and Arctic sea ice anomalies in the previous September, October, November and September–October, respectively, for the period of 1979/80–2013/14

	Sep	Oct	Nov	Sep–Oct
SCF	73 %	67 %	58 %	75 %
R	0.76	0.72	0.69	0.74

However, the winter temperature anomalies in China show little covariability with the November sea ice anomalies in the Arctic (Fig. 2e, f), which can presumably be attributed to less variation of the sea ice cover in a large part of the Arctic in November (Fig. 1c, f).

These results reveal that a close relationship exists between the winter temperature anomalies in China and autumn sea ice anomalies in the Arctic. In particular, the dominant mode of winter temperature anomalies in China is closely related to the September–October sea ice anomalies on the Eurasian side of the Arctic. A sea ice index that

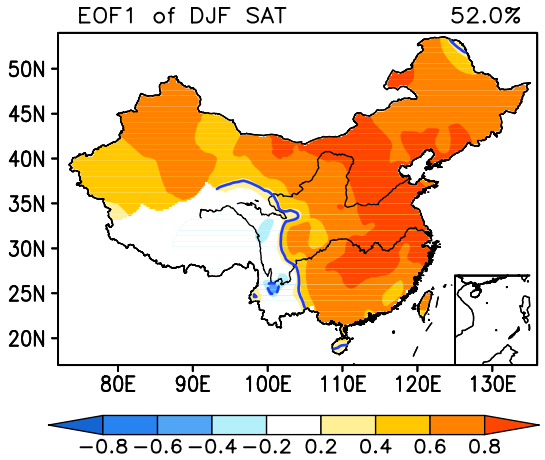

Fig. 4 Spatial pattern of the first EOF mode of detrended winter temperature anomalies in China for the period of 1979/80–2013/14. The *pattern* is represented as correlation between associated principal component and temperature anomalies, and percentage of explained variance from the pattern is given in the *right top*. *Contour* indicates significance at the 95 % confidence level

Table 2 Correlations among the sea ice indices in different autumn months for the period of 1979–2013

	Sep	Oct	Nov
Sep–Oct	0.91	0.96	0.55
Sep	\	0.75	0.42
Oct	\	\	0.59

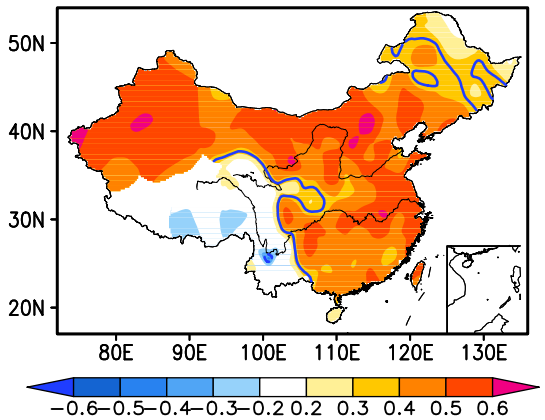

Fig. 5 Correlations between detrended winter temperature anomalies in China and the autumn sea ice index for the period of 1979/80–2013/14. *Blue contour* indicates significance at the 95 % confidence level

represents sea ice variations in the Eurasian Arctic is constructed as the regional-averaged sea ice concentrations over 72.5°–83.5°N and 30.5°–149.5°E (see box in Fig. 2d). It is found that the correlation between September and

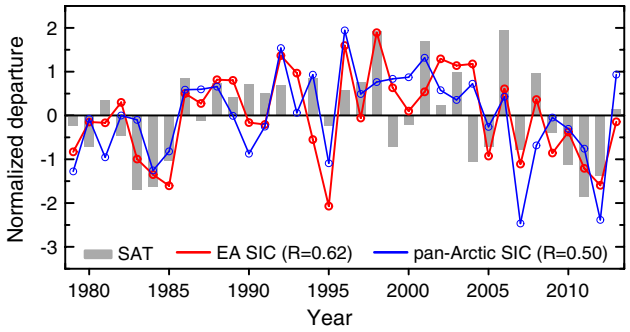

Fig. 6 Time series of the normalized first principal component of detrended winter temperature anomalies in China (*grey bar*) and autumn Eurasian Arctic sea ice (*red line*) and autumn pan-Arctic sea ice anomalies (*blue line*) during the period of 1979/80–2013/14. *R* is the correlation coefficient between the temperature and sea ice indices

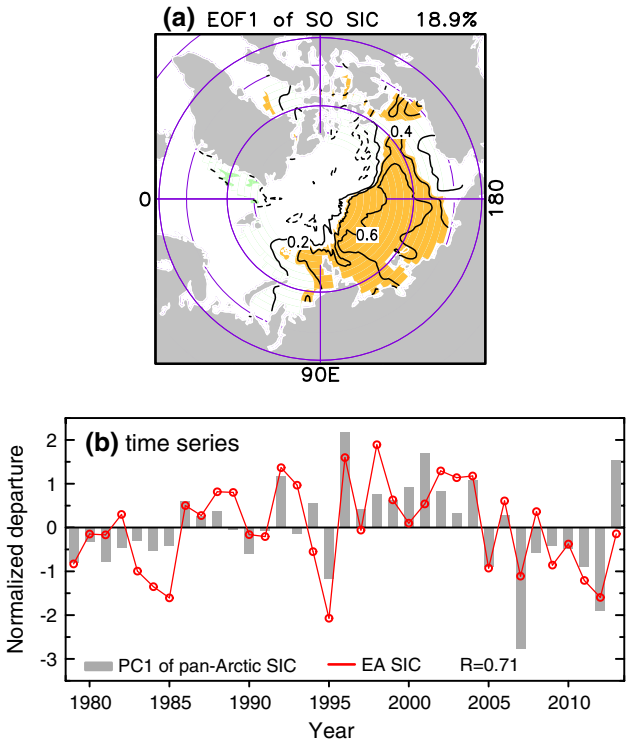

Fig. 7 **a** The same as Fig. 4, but for the autumn sea ice anomalies in the Arctic. **b** Time series of the corresponding principal component (*grey bar*) and the Eurasian Arctic sea ice anomaly (*red line*)

October sea ice indices is 0.75, which is significantly higher than their correlations with the November sea ice index (Table 2). This indicates that the September and October sea ice indices are highly correlated, but they are relatively independent of the November sea ice. Further examination indicates that the SVD patterns identified using winter temperature anomalies in China and mean September–October sea ice anomalies in the Arctic (Figure not shown) highly resemble those for using September and October sea ice anomalies separately (Fig. 2a–d). Therefore, we mainly focus on the Sep–Oct mean (hereafter, simply autumn) Arctic sea ice in the following analysis.

As shown in Fig. 5, the autumn sea ice index is significantly correlated with the winter temperature anomalies in a large part of China, which is quite consistent with the SVD results revealed in Fig. 2a–d. Furthermore, a significantly in-phase relationship can be clearly observed between the autumn sea ice index and the first principal component (PC1) of winter temperature anomalies in China (Fig. 6). Their correlation coefficient is approximately 0.62, exceeding significance at the 99 % confidence level. This indicates that the autumn sea ice index shares approximately 38 % of the covariance with the PC1 of winter temperature anomalies in China.

For comparison, we also calculate the regional-averaged sea ice concentration anomalies in the Arctic poleward of 60°N. It is shown that the PC1 of winter temperature anomalies in China has a correlation of 0.50 with the autumn pan-Arctic sea ice anomaly (Fig. 6), which is obviously lower than the correlation (0.62) with the constructed autumn sea ice index. Moreover, the identified sea ice patterns in the SVD analysis (Fig. 2b, d) are somewhat different from the first leading EOF pattern of detrended autumn sea ice anomalies in the Arctic (Fig. 7a). The corresponding principal component has a correlation of about 0.71 with the constructed autumn sea ice index (Fig. 7b) and about 0.49 with the PC1 of winter temperature in China. Therefore, these results confirm the primary importance of Eurasian Arctic sea ice anomalies in influencing winter temperature in China.

4 Atmospheric teleconnections linking Arctic to China in winter

4.1 Winter atmospheric circulation

In the previous section, we revealed that an intimately in-phase relationship exists between winter temperature anomalies in China and autumn sea ice anomalies in the Eurasian Arctic. To explore the possible mechanism responsible for this relationship, we apply correlation/regression analysis to investigate the association between winter atmospheric circulation anomalies over the Northern Hemisphere and the constructed autumn sea ice index.

As clearly shown in Fig. 8a, when the Arctic sea ice decreases in autumn, significant and positive SLP anomalies occur in the region from the Norwegian–Barents seas through Eastern Europe to Siberia and Mongolia in the following winter, indicating an enhanced SH. Consequently,

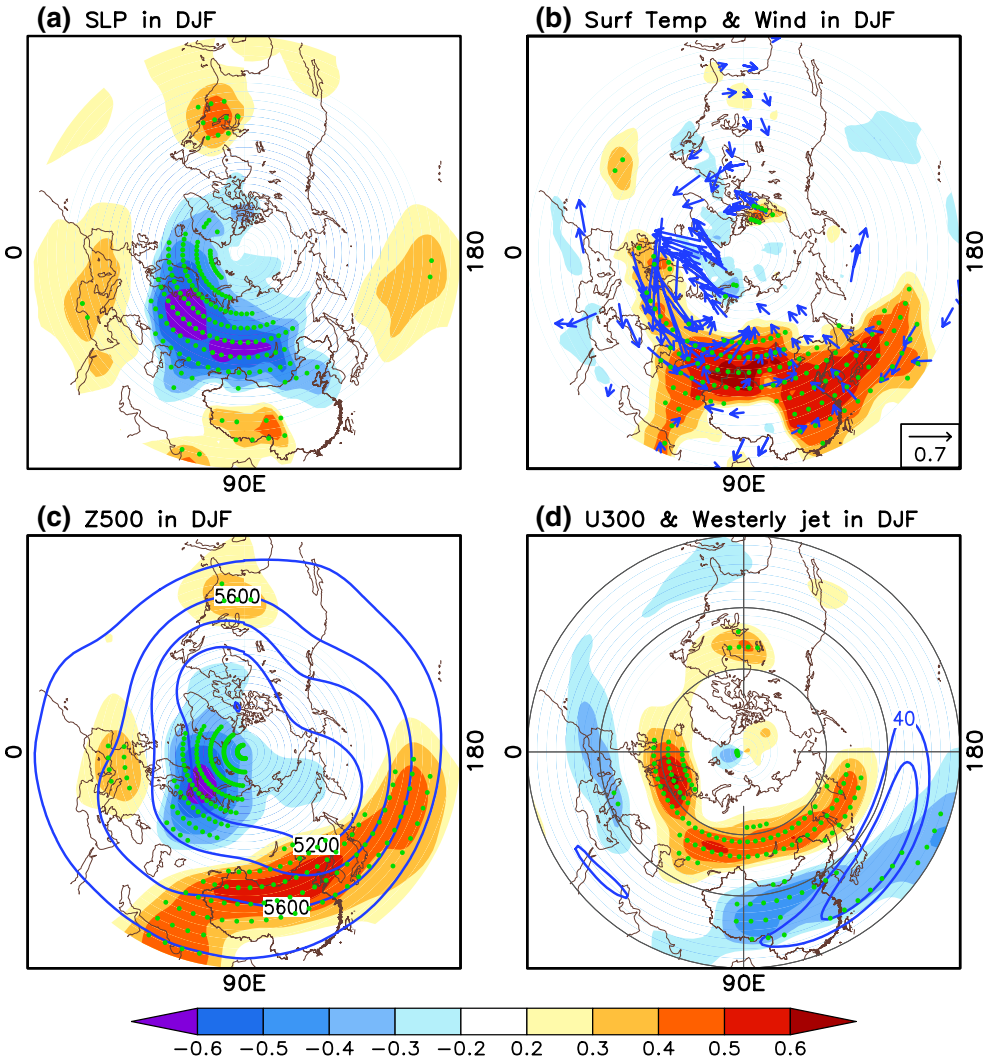

Fig. 8 Correlations (*shading*) between the detrended autumn sea ice index and winter **a** SLP, **b** surface air temperature, **c** 500-hPa geopotential height and **d** 300-hPa zonal wind anomalies for the period of 1979/80–2013/14. *Dots* indicate significance at the 95 % confidence level. *Vectors* in (**b**) denote regressed surface wind anomalies (unit: m s^{-1}) with significance at the 95 % confidence level. *Contours* in (**c**) and (**d**) represent climatological mean of 500-hPa geopotential height (unit: gpm) and 300-hPa zonal wind (unit: m s^{-1}), respectively

there are strong surface northerly anomalies east of the anomalous high pressure (Fig. 8b), which tend to enhance the cold surge activities over East Asia and favor the southward invasion of high-latitude cold air mass into China (Ding 1990). In addition, the 500-hPa geopotential height anomalies in the middle latitudes of the Asian–northwest Pacific region are significantly lower than normal (Fig. 8c), which enhances the East Asian coastal trough in the middle troposphere and thus favors further southward invasion of high-latitude cold air mass. Therefore, the surface temperature becomes colder than normal over Central and East Asia (Figs. 5, 8b). In addition, because the climatological air temperature decreases toward the east over Eurasian mid-latitudes (Nakamura et al. 2015, see their Fig. 7), the easterly anomalies south of the anomalous high pressure tend to bring cold air to Mongolia and part of China. An opposite situation can be seen when the Arctic sea ice increases in autumn. These results suggest that the impact of autumn Arctic sea ice on the following winter temperature in China appears to be related to changes in the SH and the East Asian coastal trough, both of which are large–scale atmospheric circulation systems dominating East Asian winter climate variability (Wu and Wang 2002).

Note that the pattern of winter SLP anomalies associated with the high (low) index phase of the autumn sea ice index somewhat resembles the patterns in the positive (negative) phase of the winter AO, which is characterized by positive (negative) SLP anomalies in the middle latitudes of the Northern Hemisphere and negative (positive) SLP anomalies in the Arctic (Thompson and Wallace 1998).

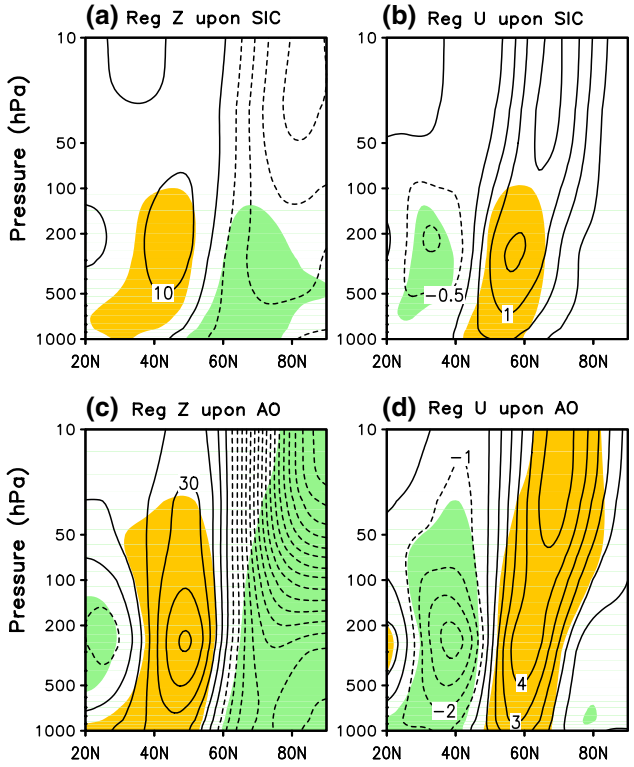

Fig. 9 Regressions of the winter **a** zonal-mean geopotential height (unit: gpm) and **b** zonal wind (unit: m s^{-1}) anomalies upon the detrended autumn sea ice index for the period of 1979/80–2013/14. **c**, **d** the same as **a**, **b**, but for the winter AO index. *Shading* indicates significance at the 95 % confidence level. The zonal mean in (**a**, **b**) covers the longitudes from 0°E to 150°E and in (**c**, **d**) from 0°E to 360°E

The AO-like pattern is clearer in the winter 500-hPa geopotential height (Fig. 8c) and 300-hPa zonal wind (Fig. 8d) anomalies regressed onto the autumn sea ice index. However, as clearly shown in Fig. 8, the strong signatures of autumn sea ice anomalies in the following winter atmospheric circulation are primarily confined to the Eastern Hemisphere, while the winter circulation anomalies associated with the autumn sea ice index are fairly weak in the middle latitudes of the North Atlantic and eastern Pacific. In other words, the typical spatial features of the winter circulation anomalies associated with the autumn Arctic sea ice anomalies are clearly distinct from the canonical winter AO pattern, and this observation is consistent with that of previous studies (Liu et al. 2012; Mori et al. 2014).

Further examinations are conducted for the vertical structures of winter circulation anomalies associated with the autumn Arctic sea ice anomalies. As shown in Fig. 9a, which is the pressure-latitude section of winter geopotential height anomaly averaged over the Eurasian sector of the Northern Hemisphere (0°–150°E) and regressed onto the autumn sea ice index, there is a meridional dipole from the surface to the lower stratosphere appearing in the mid-high latitudes of the Northern Hemisphere. A similar dipole is observed in the winter 0°–150°E zonal-mean zonal wind anomalies regressed onto the autumn sea ice index (Fig. 9b). We also examine the vertical structure of the winter 0°–360°E zonal-mean circulation anomalies associated with the autumn sea ice index (Figures not shown), and obtain similar results to those for the 0°–150°E zonal-mean. The dipole-like patterns of these anomalies somewhat resemble the vertical structure of the winter AO, which is represented by the anomalies of winter 0°–360°E zonal-mean geopotential height and zonal wind regressed onto the winter AO index (Fig. 9c, d). However, the winter circulation anomalies related to the autumn sea ice index are primarily confined to the troposphere, whereas those associated with the winter AO index could extend from the surface upward into the lower stratosphere. These results further support the conclusion regarding the different spatial features of the winter circulation anomalies associated with the autumn Arctic sea ice anomalies in comparison with the canonical winter AO pattern.

In summary, our diagnostic results show that the impacts of autumn Arctic sea ice anomalies on the following winter temperature in China appear to depend on changes in the SH and East Asian coastal trough. The winter atmospheric circulation anomalies associated with the autumn Arctic sea ice variations show a nearly annular structure over the Northern Hemisphere; however, significant circulation anomalies are primarily confined to the tropospheric Eastern Hemisphere, which clearly differ from the classical winter AO pattern. The SH and AO are the most important factors dominating winter climate variability in China, and they appear to be relatively independent of each other in influencing the East Asian winter temperature variability (Wu and Wang 2002). Thus, we further examine the roles of the SH and AO in linking autumn Arctic sea ice to winter temperature in China in the following subsection.

4.2 Relative roles of Siberian High and Arctic Oscillation

As shown in Table 3, the relationship between winter SH and AO indices is very weak ($R = -0.14$), which is consistent with the result obtained by Wu and Wang (2002). The correlation between autumn sea ice and winter SH indices is −0.59, the absolute value of which is obviously higher than that between the former and the winter AO index ($R = 0.42$). In other words, the autumn sea ice index can explain approximately 35 % of the covariance with the winter SH index but only approximately 18 % with the winter AO index. In addition, such relationships are reexamined

Table 3 Correlations among the first principal component of detrended winter temperature anomalies in China (SAT_PC1), the winter Siberian High (SH), winter AO and NAO indices and the detrended autumn (September–October) sea ice index for the period of 1979/80–2013/14

	SO sea ice	DJF SH	DJF AO	DJF NAO
DJF SH	–0.59**	/	/	/
DJF AO	0.42*	–0.14	/	/
DJF NAO	0.28	0.16	0.77**	/
DJF SAT_PC1	0.62**	–0.74**	0.33	0.03

The correlation coefficient exceeding the 95 and 99 % confidence level is indicated by * and **, respectively

by only changing the winter AO index into the winter NAO index, and a similar conclusion can be obtained (Table 3).

To further clarify the role of winter SH (AO) in linking the winter temperature anomalies in China to the autumn Arctic sea ice anomalies, we compare correlations between the autumn sea ice index and the original winter temperature anomalies in China with correlations calculated with the residual temperature anomalies after removing the winter SH (AO) signal from the data. Here, the SH (AO) signal is removed by applying a linear regression of temperature anomalies onto the SH (AO) index. As shown in Fig. 5a, significant and positive correlations exist between the autumn sea ice index and the original winter temperature anomalies in a large part of China, except in the Tibetan Plateau and part of northeastern China. However, these significant correlations between the autumn sea ice index and the winter temperature anomalies in China nearly vanish after removing the winter SH signal (Fig. 10a). In contrast, the pattern of correlations between autumn sea ice index and winter temperature anomalies in China shows only little change after removing the winter AO signal, except that the positive correlations decrease in northern China (Fig. 10b). Moreover, the PC1 of winter temperature anomalies in China, which is significantly correlated with the autumn sea ice index, has a relatively low correlation with the winter AO index ($R = 0.33$) but is highly correlated with the winter SH index ($R = -0.74$) (Table 3). These results confirm the vital role of the SH, rather than the AO, in linking winter temperature anomalies in China to autumn Arctic sea ice anomalies.

5 Empirical prediction of winter temperature anomalies in China

To further investigate the potential predictability of winter temperature anomalies in China from the autumn Arctic sea ice anomalies, a statistical prediction model is designed for the temperature in each station using the constructed autumn sea ice index as the predictor in a linear regression equation. We use leave-one-out cross-validation and independent validation methods to assess the potential predictability of the model. For the independent validation, the prediction model is trained using all observations for the period of 1979/80 to the year preceding the target year. We calculate the anomalous correlation between the observation and prediction as the skill score for evaluating the model's performance.

Figure 11a and b show the correlation skills of winter temperature anomalies in China predicted by the autumn sea ice index for cross-validation during 1979/80–2013/14 (35 years) and independent validation during 1997/98–2013/14 (17 years), respectively. Clearly, the pattern of correlation skills for cross-validation is quite consistent with that of the independent validation. Highly positive correlations can be observed in a large part of China, particularly in northwestern and central China. The correlation skill is as high as 0.60 for the PC1 of winter temperature anomalies in China for cross-validation during 1979/80–2013/14 (Fig. 12). Moreover, the skill patterns in Fig. 11a and b also resemble the correlation map between winter temperature anomalies in China and autumn sea ice index shown in

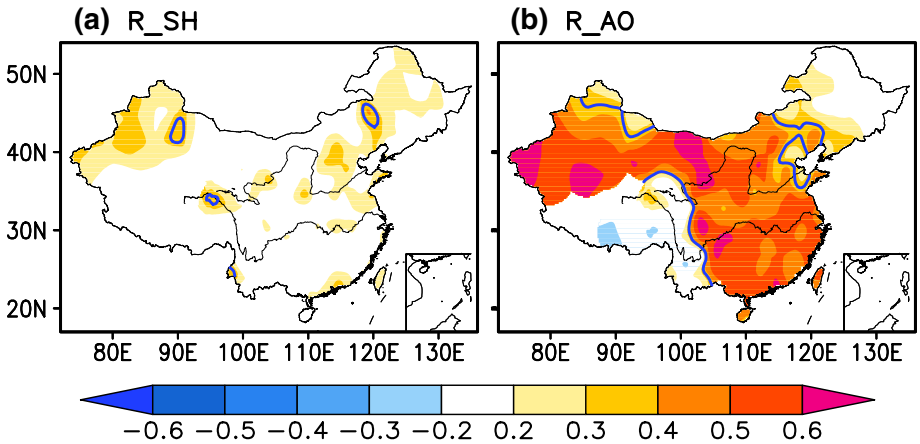

Fig. 10 The same as Fig. 5, but for the residual temperature anomalies after removing the signals of winter **a** Siberian High and **b** AO from the data, respectively

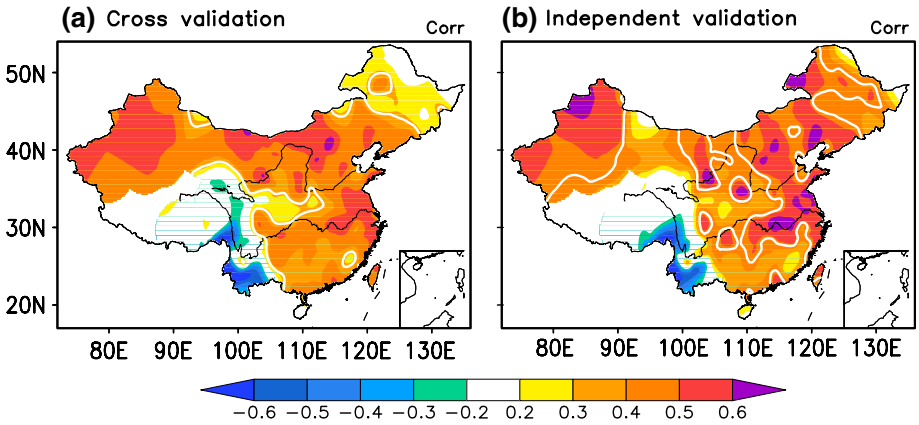

Fig. 11 Correlation skills of the winter temperature anomalies predicted by the autumn sea ice index for **a** cross validation during 1979/80–2013/14 and **b** independent validation during 1997/98–2013/14. Regions enclosed in *white contour* exceed significance at the 90 % confidence level

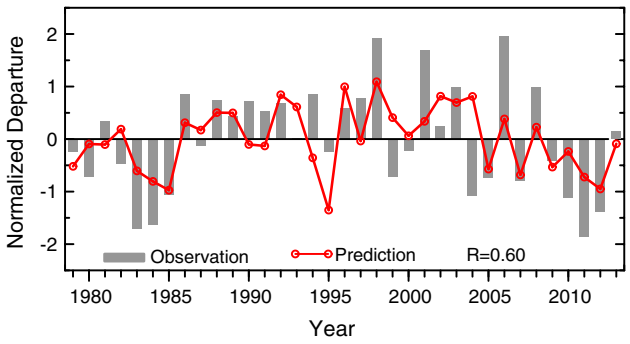

Fig. 12 Time series of the normalized first principal component of detrended winter temperature anomalies in China for observation and prediction in the cross-validation test during 1979/80–2013/14. *R* denotes correlation between the observation and prediction

Fig. 5. These results suggest that there is considerable skill in the empirical prediction of winter temperature anomalies in China from autumn Arctic sea ice variations.

In addition, the spatial anomaly correlation coefficient (ACC) between the observational and predicted detrended temperature anomalies for all of China is estimated for each winter. The temperature anomalies are normalized by the observational standard deviation prior to calculating the ACC. As shown in Fig. 13, for the majority of winters, the statistical model can give positive spatial ACC skills in predicting winter temperature anomalies in China from the autumn sea ice index. There are six (one) out of 17 winters with an ACC skill greater (less) than 0.4 (−0.4) for the independent validation and ten (four) out of 35 winters for the cross-validation. This confirms that substantial predictability of winter temperature anomalies in China can be extracted from the autumn Arctic sea ice conditions. However, it should be noticed that the performance of the autumn Arctic sea ice index as a proxy for the winter temperature anomalies in China is not good in some years. This is primarily because the winter temperature variability in China is not only influenced by the Arctic sea ice anomalies but also by other factors, such as tropical eastern Pacific sea surface temperature anomalies.

6 Summary and discussion

We have investigated the large–scale patterns of interannual covariability between winter temperature anomalies in China and the previous autumn sea ice anomalies in the Arctic using an SVD technique to understand the main features of and mechanism underlying autumn Arctic sea ice in influencing winter China temperature variability. Based on monthly observations and reanalysis dataset for the period of 1979–2014, our analysis results showed that a

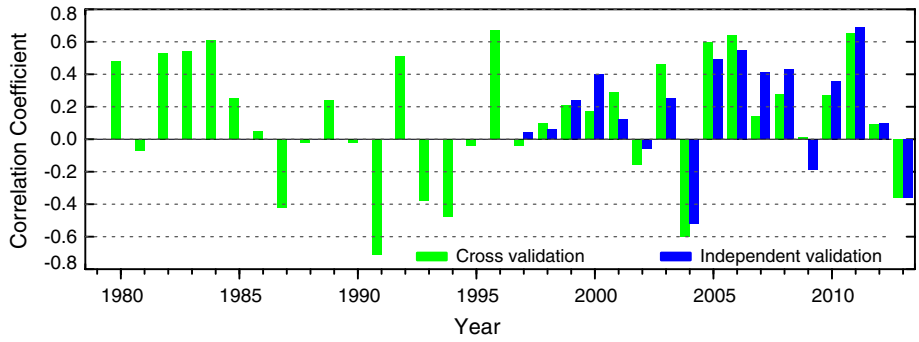

Fig. 13 Spatial ACC skills of normalized winter temperature anomalies in China predicted by the autumn sea ice index for cross validation during 1979/80–2013/14 and independent validation during 1997/98–2013/14

close relationship exists between the autumn (September–October) sea ice anomalies in the Eurasian Arctic and the following winter temperature anomalies in a large part of China. The reduced (increased) sea ice anomalies tend to be followed by cold (warm) winter temperature anomalies in China, except in the Tibetan Plateau, indicating that the autumn Arctic sea ice anomalies evidently contribute to the formation of the dominant pattern of winter temperature variability in China. We also found that the autumn Arctic sea ice anomalies can explain approximately 38 % of the variance of the dominant component of winter temperature anomalies in China for the period of 1979/80–2013/14.

Our observational analysis indicated that the impacts of the autumn Arctic sea ice anomalies on the following winter temperature anomalies in China are closely linked to the large–scale atmospheric circulation anomalies over Eurasia. When the autumn sea ice anomalies are lower than normal in the Eurasian Arctic, high-pressure anomalies appear to prevail over the region from the Barents Sea to Eastern Europe and Mongolia and below-normal 500-hPa geopotential height anomalies occur over the middle latitudes of the Asian-western Pacific region in the following winter. These results indicate that the winter SH and East Asia coastal trough are preferentially strengthened, which favor a southward invasion of high-latitude cold air masses and result in cold temperature anomalies in a large part of China. An opposite scenario can be observed when the autumn sea ice anomalies become higher than normal in the Eurasian Arctic.

Many previous studies have revealed that the pattern of winter atmospheric circulation anomalies associated with the autumn and winter Arctic sea ice anomalies tends to resemble the AO/NAO pattern (Deser et al. 2007; Wu and Zhang 2010; Kim et al. 2014; Nakamura et al. 2015). However, we found that significant changes in the winter atmospheric circulation associated with the autumn sea ice anomalies in the Eurasian Arctic are primarily confined to the tropospheric Eastern Hemisphere, which is clearly differential from the classical winter AO-related circulation pattern typically characterized by a more zonal-symmetric structure from the surface to the lower stratosphere (Thompson and Wallace 1998). This is consistent with the study of Mori et al. (2014), who demonstrated from observations and 100-member ensembles of atmospheric general circulation simulations that the winter atmospheric response to autumn sea ice decline in the Barents–Kara sea is approximately independent of the AO.

Moreover, we have shown that the significantly in-phase relationship between the autumn Arctic sea ice anomalies and the following winter temperature anomalies in China nearly vanishes after linearly removing the signal of winter SH from the data. However, their pattern shows little change after removing the winter AO signal. This indicates that the impact of autumn Arctic sea ice anomalies on the winter temperature anomalies in China strongly depends on the winter SH variability. In other words, the SH plays a crucial role in delivering the effects of the autumn Arctic sea ice anomalies on the winter China temperature variability. Numerical experiments designed by Wu et al. (2011) have confirmed the intimate relationship between the winter SH and autumn Arctic sea ice anomalies, supporting our conclusion regarding the role of winter SH in linking winter temperature anomalies in China to autumn Arctic sea ice variability.

Based on this evidence, we further examined the potential predictability of winter temperature anomalies in China from the autumn Arctic sea ice anomalies by developing a statistical prediction model in which only the autumn sea ice anomalies in the Eurasian Arctic are used as a predictor in a linear regression equation. Results from both cross-validation and independent validation revealed that the model shows considerable hindcast skill for winter temperature anomalies over a large part of China, particularly northwestern and central China. In addition, in most winters, the model gave skillful predictions of temperature anomalies in China by extracting only predictability from the autumn Arctic sea ice variations. Therefore, the autumn Arctic sea ice anomalies could act as an important predictor for the following winter temperature anomalies in a large part of China. This indicates a significant potential for further improving winter China climate prediction on the basis of the autumn Arctic sea ice variability.

The robust effects of autumn Arctic sea ice anomalies on the following winter atmospheric circulation and surface climate variability in the extratropical Northern Hemisphere have been demonstrated by many numerical studies (e.g., Honda et al. 2009; Liu et al. 2012; Mori et al. 2014). Some studies suggested that the delayed atmospheric circulation response to the autumn Arctic sea ice anomalies is possibly related to the persistence of sea ice anomalies and the associated changes in local sea surface temperature, snow cover and cloudiness from autumn to winter (e.g., Francis et al. 2009; Honda et al. 2009; Wu et al. 2011). Other studies revealed that the stratosphere-troposphere coupling plays a role in linking the late autumn Arctic sea ice anomalies and winter climate variability in the Northern Hemisphere (e.g., Kim et al. 2014; Nakamura et al. 2015). However, we found in this study that the signal of early-mid autumn sea ice anomalies in the Eurasian Arctic is primarily confined to the troposphere. These indicate that physical mechanisms responsible for the linkage of winter climate variability in the Northern Hemisphere to the early-mid autumn Arctic sea ice anomalies may somewhat differ from those for the late autumn Arctic sea ice anomalies, which needs to be investigated in further studies. Although different mechanisms have been proposed for such linkage (Francis et al. 2009; Honda

et al. 2009; Francis and Vavrus 2012; Kim et al. 2014), the detailed physical processes are still not clear and subject to uncertainties, particularly under the conditions of quite deficient observational data in the Arctic and large model sensitivities and intrinsic variability (Screen et al. 2013), which is beyond the scope of this study. Nevertheless, our results suggested that autumn Arctic sea ice anomalies could provide an important source for the skillful prediction of the following winter temperature anomalies in China.

Acknowledgments This work is jointly supported by the 973 Program of China (2013CB430203), the National Natural Science Foundation of China (41205058 and 41375062), the China meteorological special project (GYHY201406022), and the open funding of LCS/CMA. The authors are grateful to two anonymous reviewers for their insightful comments to improve the quality of the paper.

References

Alexander MA, Bhatt US, Walsh JE (2004) The atmospheric response to realistic sea ice anomalies in an AGCM during winter. J Clim 17:890–905

Bader J, Mesquita MDS, Hodges KI, Keenlyside N, Østerhus S, Miles M (2011) A review on Northern Hemisphere sea-ice, storminess and the North Atlantic Oscillation: observations and projected changes. Atmos Res 101:809–834. doi:10.1016/j.atmosres.2011.04.007

Barnston AG, Livezey RE (1987) Classification, seasonality and persistence of low-frequency atmospheric circulation patterns. Mon Weather Rev 115:1083–1126

Budikova D (2009) Role of Arctic sea ice in global atmospheric circulation: a review. Glob Planet Change 68:149–163. doi:10.1016/j.gloplacha.2009.04.001

Comiso JC (2012) Large decadal decline of the Arctic multiyear ice cover. J Clim 25:1176–1193. doi:10.1175/JCLI-D-11-00113.1

Comiso JC, Parkinson CL, Gersten R, Stock L (2008) Accelerated decline in the Arctic sea ice cover. Geophys Res Lett 35:L01703. doi:10.1029/2007GL031972

Deser C, Magnusdottir G, Saravanan R (2004) The effects of North Atlantic SST and sea ice anomalies on the winter circulation in CCM3. Part II: Direct and indirect components of the response. J Clim 17:877–889

Deser C, Tomas RA, Peng S (2007) The transient atmospheric circulation response to North Atlantic SST and sea ice anomalies. J Clim 20:4751–4767. doi:10.1175/JCLI4278.1

Ding YH (1990) Buildup, air-mass transformation and propagation of Siberian High and its relations to cold surge in East Asia. Meteorol Atmos Phys 44:281–292. doi:10.1007/BF01026822

Francis JA, Vavrus SJ (2012) Evidence linking Arctic amplification to extreme weather in mid-latitudes. Geophys Res Lett 39:L06801. doi:10.1029/2012GL051000

Francis JA, Chan W, Leathers DJ, Miller JR, Veron DE (2009) Winter Northern Hemisphere weather patterns remember summer Arctic sea-ice extent. Geophys Res Lett 36:L07503. doi:10.1029/2009GL037274

Gao YQ, Sun JQ, Li F, He SP, Sandven S, Yan Q, Zhang ZS, Lohmann K, Keenlyside N, Furevik T, Suo LL (2015) Arctic sea ice and Eurasian climate: a review. Adv Atmos Sci 32:92–114. doi:10.1007/s00376-014-0009-6

Honda M, Inous J, Yamane S (2009) Influence of low Arctic sea-ice minima on anomalously cold Eurasian winters. Geophys Res Lett 36:L08707. doi:10.1029/2008GL037079

Kanamitsu M, Ebisuzaki W, Woollen J, Yang S-K, Hnilo JJ, Fiorino M, Potter GL (2002) NCEP/DOE AMIP-II Reanalysis (R-2). Bull Am Meteorol Soc 83:1631–1643

Karl TR, Arguez A, Huang B, Lawrimore JH, McMahon JR, Menne MJ, Peterson TC, Vose RS, Zhang H-M (2015) Possible artifacts of data biases in the recent global surface warming hiatus. Science. doi:10.1126/science.aaa5632

Kim B-M, Son S-W, Min S-K, Jeong J-H, Kim S-J, Zhang X, Shim T, Yoon J-H (2014) Weakening of the stratospheric polar by Arctic sea ice loss. Nat Commun 5:4646. doi:10.1038/ncomms5646

Koenigk T, Caian M, Nikulin G, Schimanke S (2015) Regional Arctic sea ice variations as predictor for winter climate conditions. Clim Dyn. doi:10.1007/s00382-015-2586-1

Li F, Wang H (2013) Relationship between Bering Sea ice cover and East Asian winter monsoon year-to-year variations. Adv Atmos Sci 30:48–56. doi:10.1007/s00376-012-2071-2

Li J, Wu Z (2012) Importance of autumn Arctic sea ice to northern winter snowfall. Proc Natl Acad Sci USA 109:E1898. doi:10.1073/pnas.1205075109

Liu Y, Ren H-L (2015) A hybrid statistical downscaling model for prediction of winter precipitation in China. Int J Climatol 35:1309–1321. doi:10.1002/joc.4058

Liu J, Zhang Z, Horton RM, Wang C, Ren X (2007) Variability of North Pacific sea ice and East Asia–North Pacific winter climate. J Clim 20:1991–2001. doi:10.1175/JCLI4105.1

Liu J, Curry JA, Wang H, Song M, Horton RM (2012a) Impact of declining Arctic sea ice on winter snowfall. Proc Natl Acad Sci USA 109:4074–4079. doi:10.1073/pnas.1114910109

Liu N, Liu J, Zhang Z, Chen H, Song M (2012b) Is extreme Arctic sea ice anomaly in 2007 a key contributor to severe January 2008 snowstorm in China? Int J Climatol 32:2081–2087. doi:10.1002/joc.2400

Mori M, Watanabe M, Shiogama H, Inoue J, Kimoto M (2014) Robust Arctic sea-ice influence on the frequent Eurasian cold winters in past decades. Nat Geosci 7:869–873. doi:10.1038/ngeo2277

Nakamura T, Yamazaki K, Iwamoto K, Honda M, Miyoshi Y, Ogawa Y, Ukita J (2015) A negative phase shift of the winter AO/NAO due to the recent Arctic sea-ice reduction in late autumn. J Geophys Res Atmos 120:3209–3227. doi:10.1002/2014JD022848

Ogi M, Yamazaki K, Wallace JM (2010) Influence of winter and summer wind anomalies on summer Arctic sea ice extent. Geophys Res Lett 37:L07701. doi:10.1029/2009GL042356

Petoukhov V, Semenov VA (2010) A link between reduced Barents-Kara sea ice and cold winter extremes over northern continents. J Geophys Res 115:D21111. doi:10.1029/2009JD013568

Rayner NA, Parker DE, Horton EB, Folland CK, Alexander LV, Rowell DP, Kent EC, Kaplan A (2003) Global analyses of sea surface temperature, sea ice, and night marine air temperature since the late nineteenth century. J Geophys Res 108:4407. doi:10.1029/2002JD002670

Rinke A, Dethloff K, Dorn W, Handorf D, Moore JC (2013) Simulated Arctic atmospheric feedbacks associated with late summer sea ice anomalies. J Geophys Res 118:7698–7714. doi:10.1002/jgrd.50584

Screen JA, Simmonds I, Deser C, Tomas R (2013) The atmospheric response to three decades of observed Arctic sea ice loss. J Clim 26:1230–1248. doi:10.1175/JCLI-D-12-00063.1

Tang Q, Zhang X, Yang X, Francis JA (2013) Cold winter extremes in northern continents linked to Arctic sea ice loss. Environ Res Lett 8:014036. doi:10.1088/1748-9326/8/1/014036

Thompson DWJ, Wallace JM (1998) The Arctic Oscillation signature in the wintertime geopotential height and temperature fields. Geophys Res Lett 25:1297–1300

Vihma T (2014) Effects of Arctic sea ice decline on weather and climate: a review. Surv Geophys 35:1175–1214. doi:10.1007/s10712-014-9284-0

Wu B, Wang J (2002) Winter Arctic Oscillation, Siberian High and East Asian winter monsoon. Geophys Res Lett 29:1897. doi:10.1029/2002GL015373

Wu QG, Zhang XD (2010) Observed forcing-feedback processes between Northern Hemisphere atmospheric circulation and Arctic sea ice coverage. J Geophys Res 115:D14119. doi:10.1029/2009JD013574

Wu B, Huang R, Gao D (1999) The impact of variation of sea-ice extent in the Kara Sea and the Barents Sea in winter on the winter monsoon over East Asia (in Chinese). Chin J Atmos Sci 23:267–275

Wu B, Su J, Zhang R (2011a) Effects of autumn–winter Arctic sea ice on winter Siberian High. Chin Sci Bull 56:3220–3228. doi:10.1007/s11434-011-4696-4

Wu Z, Li J, Jiang Z, He J (2011b) Predictable climate dynamics of abnormal East Asian winter monsoon: once-in-a-century snowstorms in 2007/2008 winter. Clim Dyn 37:1661–1669. doi:10.1007/s00382-010-0938-4

Wu B, Overland JE, D'Arrigo R (2012) Anomalous Arctic surface wind patterns and their impacts on September sea ice minima and trend. Tellus 64:18590. doi:10.3402/tellusa.v64i0.18590

Wu B, Handorf D, Dethloff K, Rinke A, Hu A (2013) Winter weather patterns over Northern Eurasia and Arctic sea ice loss. Mon Weather Rev 141:3786–3800. doi:10.1175/MWR-D-13-00046.1

Zwiers FW, von Storch H (1995) Taking serial correlation into account in tests of the mean. J Clim 8:336–351. doi:10.1175/1520-0442(1995)008<0336:TSCIAI>2.0.CO;2